

Hybrid Quantum–Classical Decoder Transformer

Sumant Ravi

1 Overview

This project explores a **hybrid quantum–classical decoder-only Transformer** in which the classical **Feed-Forward Network (FFN)** inside each Transformer block is replaced with a **Quantum Neural Network (QNN)**.

The model is implemented using **PyTorch** and **PennyLane** and trained end-to-end with gradient-based optimization.

2 Decoder-Only Transformer (Causal Self-Attention)

Let the input sequence of hidden states be

$$X \in \mathbb{R}^{T \times d_{\text{model}}}. \quad (1)$$

2.1 Linear Projections

Queries, keys, and values are computed via

$$Q = XW_Q, \quad K = XW_K, \quad V = XW_V, \quad (2)$$

where

$$W_Q, W_K, W_V \in \mathbb{R}^{d_{\text{model}} \times d_h}. \quad (3)$$

2.2 Scaled Dot-Product Attention

The attention score matrix is

$$S = \frac{1}{\sqrt{d_h}} QK^\top \in \mathbb{R}^{T \times T}. \quad (4)$$

2.3 Causal Masking

To enforce autoregressive decoding:

$$S_{ij} = -\infty \quad \text{for } j > i. \quad (5)$$

2.4 Attention Weights and Output

$$A = \text{softmax}(S), \quad (6)$$

$$Z = AV \in \mathbb{R}^{T \times d_h}. \quad (7)$$

3 Multi-Head Attention

For H heads, with $d_h = d_{\text{model}}/H$, for head $h = 1, \dots, H$:

$$Q^{(h)} = XW_Q^{(h)}, \quad K^{(h)} = XW_K^{(h)}, \quad V^{(h)} = XW_V^{(h)}, \quad (8)$$

with

$$W_Q^{(h)}, W_K^{(h)}, W_V^{(h)} \in \mathbb{R}^{d_{\text{model}} \times d_h}. \quad (9)$$

Per-head attention:

$$S^{(h)} = \frac{1}{\sqrt{d_h}} Q^{(h)} (K^{(h)})^\top, \quad (10)$$

$$S_{ij}^{(h)} = -\infty \quad \text{for } j > i, \quad (11)$$

$$A^{(h)} = \text{softmax}(S^{(h)}), \quad (12)$$

$$Z^{(h)} = A^{(h)} V^{(h)} \in \mathbb{R}^{T \times d_h}. \quad (13)$$

Concatenate and project:

$$Z_{\text{concat}} = [Z^{(1)} \| Z^{(2)} \| \dots \| Z^{(H)}] \in \mathbb{R}^{T \times d_{\text{model}}}, \quad (14)$$

$$Y = Z_{\text{concat}} W_O, \quad W_O \in \mathbb{R}^{d_{\text{model}} \times d_{\text{model}}}. \quad (15)$$

Residual + LayerNorm:

$$X_{\text{res1}} = X + Y, \quad (16)$$

$$H = \text{LayerNorm}(X_{\text{res1}}), \quad H \in \mathbb{R}^{T \times d_{\text{model}}}. \quad (17)$$

4 Classical Feed-Forward Network (Baseline)

The classical FFN is

$$\phi_{\text{classical}} : \mathbb{R}^{d_{\text{model}}} \rightarrow \mathbb{R}^{d_{\text{model}}}, \quad (18)$$

and is typically implemented as

$$\phi_{\text{classical}}(x) = W_2 \sigma(W_1 x + b_1) + b_2, \quad (19)$$

with the shape transformation

$$\mathbb{R}^{d_{\text{model}}} \rightarrow \mathbb{R}^{d_{\text{ff}}} \rightarrow \mathbb{R}^{d_{\text{model}}}. \quad (20)$$

5 Quantum Neural Network (QNN) Replacement

We replace the FFN with a QNN operating on M qubits, using:

- a classical pre-projection to dimension M ,
- angle encoding into a quantum state,
- a parameterized quantum circuit with rotation + entanglement layers,
- Pauli-Z expectation readout,
- a classical post-projection back to $\mathbb{R}^{d_{\text{model}}}$.

5.1 Classical Pre-Projection (to match # qubits)

Let $x \in \mathbb{R}^{d_{\text{model}}}$ be a token's hidden state. Define

$$z = W_{\text{in}}x + b_{\text{in}} \in \mathbb{R}^M. \quad (21)$$

5.2 Angle Encoding

Define the encoding unitary

$$U_{\text{encode}}(z) = \bigotimes_{j=0}^{M-1} R_Y(z_j), \quad (22)$$

where

$$R_Y(\alpha) = e^{-i\alpha\sigma_Y/2}. \quad (23)$$

The input state is

$$|\psi_{\text{input}}\rangle = U_{\text{encode}}(z) |0\rangle^{\otimes M}. \quad (24)$$

5.3 Variational Rotation Layer (all qubits)

For layer ℓ , define

$$U_{\text{rot}}^{(\ell)}(\theta_\ell) = \prod_{j=0}^{M-1} [R_Y(\theta_{\ell,j,0}) R_Z(\theta_{\ell,j,1}) R_Y(\theta_{\ell,j,2})], \quad (25)$$

with

$$R_Z(\beta) = e^{-i\beta\sigma_Z/2}. \quad (26)$$

5.4 Entanglement Operator (Ring)

Define the ring entanglement unitary

$$U_{\text{ent}}^{(\ell)} = \prod_{j=0}^{M-1} \text{CNOT}(j, (j+1) \bmod M). \quad (27)$$

This forms a circular entanglement pattern:

$$0 \rightarrow 1 \rightarrow \dots \rightarrow M-1 \rightarrow 0.$$

5.5 One Layer and Full Circuit

One QNN layer is

$$U^{(\ell)}(\theta^\ell) = U_{\text{ent}}^{(\ell)} U_{\text{rot}}^{(\ell)}(\theta_\ell). \quad (28)$$

The full circuit with L layers is

$$U(\theta) = \prod_{\ell=0}^{L-1} U^{(\ell)}(\theta^\ell). \quad (29)$$

5.6 Final State

$$|\psi_{\text{final}}(x, \theta)\rangle = U(\theta) U_{\text{encode}}(z) |0\rangle^{\otimes M}. \quad (30)$$

5.7 Measurement Output (Pauli-Z Expectations)

The QNN output vector is

$$\mu(x, \theta) = (\langle Z_1 \rangle, \langle Z_2 \rangle, \dots, \langle Z_M \rangle) \in [-1, 1]^M, \quad (31)$$

where each component is

$$\langle Z_j \rangle = \langle \psi_{\text{final}}(x, \theta) | Z_j | \psi_{\text{final}}(x, \theta) \rangle. \quad (32)$$

5.8 Classical Readout Back to Model Dimension

$$\phi_{\text{QNN}}(x) = W_{\text{out}} \mu(x, \theta) + b_{\text{out}} \in \mathbb{R}^{d_{\text{model}}}. \quad (33)$$

5.9 Key Idea (Hilbert Space Dimension)

$$\dim(\mathcal{H}) = 2^M. \quad (34)$$

6 Hidden States to Probability Distribution

After all Transformer blocks and a final LayerNorm, the model produces a hidden state for each token position:

$$h(t) \in \mathbb{R}^{d_{\text{model}}}, \quad t = 1, \dots, T. \quad (35)$$

The hidden state is mapped to vocabulary logits via a linear projection:

$$\text{logits}(t) = W_{\text{lm}} h(t), \quad (36)$$

where

$$W_{\text{lm}} \in \mathbb{R}^{V \times d_{\text{model}}}, \quad (37)$$

and V is the vocabulary size.

Applying softmax produces a probability distribution over the vocabulary:

$$p(t) = \text{softmax}(\text{logits}(t)) \in \mathbb{R}^V. \quad (38)$$

7 Autoregressive Text Generation

Final block output:

$$H \in \mathbb{R}^{T \times d_{\text{model}}}, \quad (39)$$

where the row

$$H_t \in \mathbb{R}^{d_{\text{model}}} \quad (40)$$

is the hidden representation of the first t tokens.

At generation time, only the last hidden state is used:

$$h_{\text{last}} = H_T \in \mathbb{R}^{d_{\text{model}}}. \quad (41)$$

The model computes vocabulary logits:

$$\text{logits} = h_{\text{last}} W_{\text{lm}}^\top \in \mathbb{R}^V. \quad (42)$$

Applying softmax gives the probability distribution for the next token. A new token is selected by either sampling or argmax (implementation uses sampling).

8 Cross-Entropy Loss

The model is trained with cross-entropy loss for next-token prediction:

$$\mathcal{L}(\theta) = -\frac{1}{|B|T} \sum_{b \in B} \sum_{t=1}^T \log p_\theta(y_{b,t} | x_{b,1:t}). \quad (43)$$

Define

$$p(t) = \text{softmax}(\text{logits}(t)), \quad (44)$$

and component-wise

$$p(t)_v = \frac{\exp(\text{logits}(t)_v)}{\sum_{u=1}^V \exp(\text{logits}(t)_u)}. \quad (45)$$

Then

$$p_\theta(y_{b,t} | x_{b,1:t}) = p(t)_{y_{b,t}}, \quad (46)$$

and equivalently

$$\mathcal{L}(\theta) = -\frac{1}{|B|T} \sum_{b \in B} \sum_{t=1}^T \log(p(t)_{y_{b,t}}). \quad (47)$$

Where:

- $y_{b,t}$ is the correct next token at position t in batch b ,
- $|B|$ is batch size,
- T is context (sequence) length.

9 Model Evaluation

A 90–10 train–validation split was used (90% training, 10% validation). Main evaluation metrics are validation loss and **perplexity**.

$$\text{Perplexity} = e^{\mathcal{L}(\theta)}, \quad (48)$$

where $\mathcal{L}(\theta)$ is the cross-entropy error.

Interpretation (slide language):

- Perplexity is the model’s average branching factor.
- Can think of perplexity as “how surprised” the model is by the correct sequence.
- Low surprise → low perplexity; high surprise → high perplexity.
- Low perplexity means higher probability assigned to correct next tokens.
- High perplexity means more uncertainty spread across many wrong tokens.

10 Findings (Plots)

Upload your plots into `figures/` in Overleaf (or repo `docs/figures/` locally).

10.1 Case 1: Small Model

- Base config: $d_{\text{model}} = 32$, 2 blocks, 2 heads, max_context_length=20, dropout=0.1
- Classical model dimension $d_{\text{ff}} = 128$
- Number of qubits $M = 3$

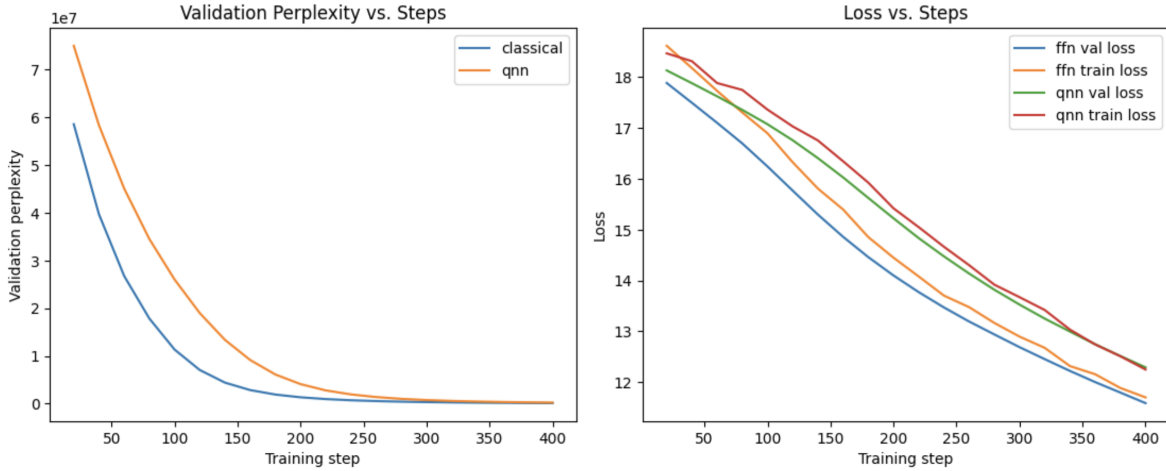


Figure 1: Case 1: Validation perplexity and loss vs steps (classical vs QNN).

10.2 Case 2: Larger Feed-Forward

- Base config: $d_{\text{model}} = 32$, 2 blocks, 2 heads, max_context_length=20, dropout=0.1
- Classical model dimension $d_{\text{ff}} = 256$
- Number of qubits $M = 4$

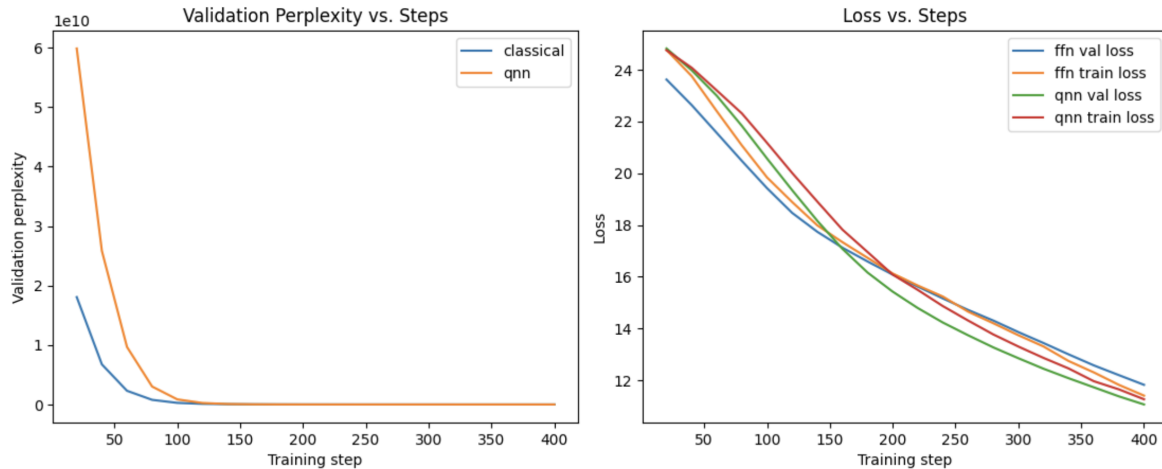


Figure 2: Case 2: Larger FFN comparison (classical vs QNN).

10.3 Case 3: Larger MHA

- Base config: $d_{\text{model}} = 128$, 4 blocks, 4 heads, max_context_length=20, dropout=0.1
- Classical model dimension $d_{\text{ff}} = 128$
- Number of qubits $M = 3$

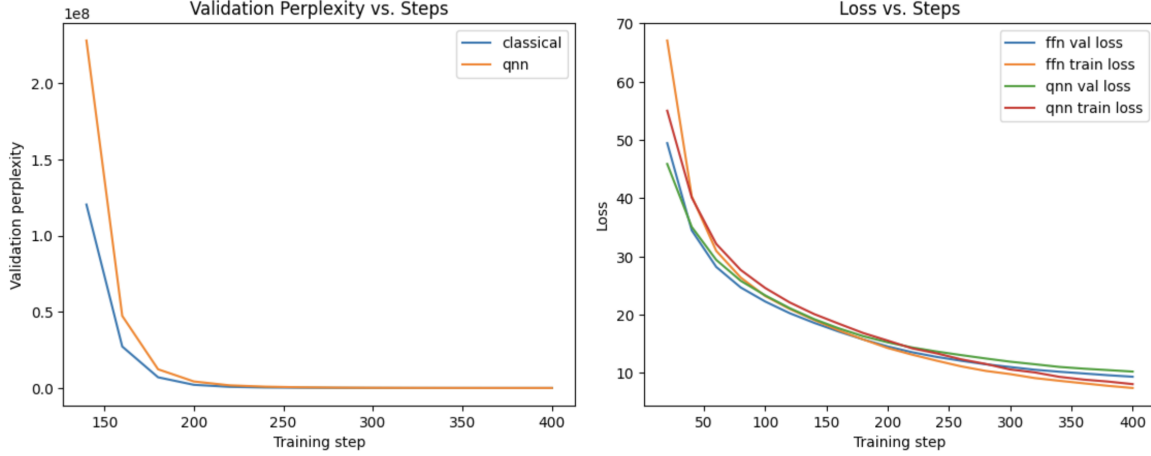


Figure 3: Case 3: Larger attention configuration (classical vs QNN).

10.4 Case 4: Bigger Model

- Base config: $d_{\text{model}} = 128$, 4 blocks, 4 heads, max_context_length=30, dropout=0.1
- Classical model dimension $d_{\text{ff}} = 256$
- Number of qubits $M = 4$

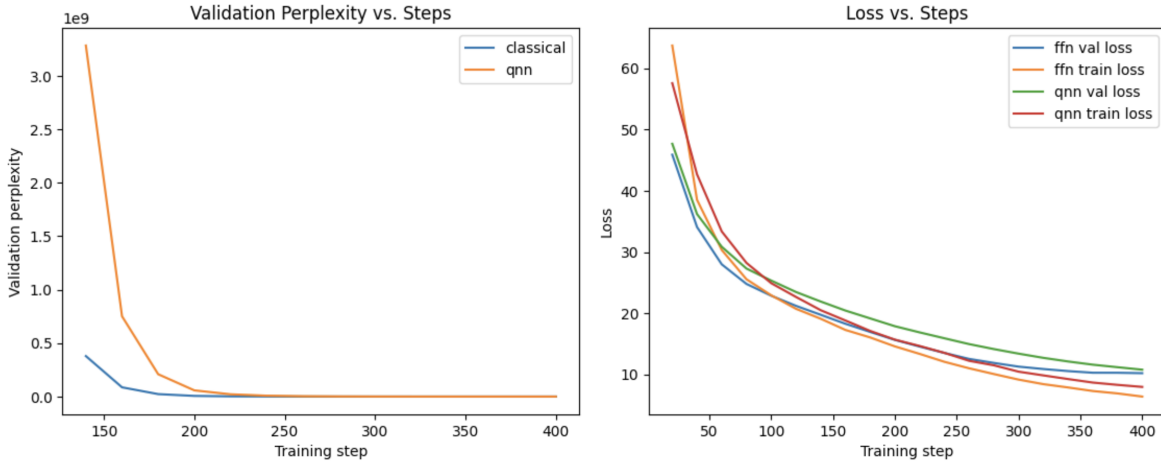


Figure 4: Case 4: Bigger model configuration (classical vs QNN).

11 Potential Advantage

11.1 Ideal

- Because multi-qubit quantum states inhabit a Hilbert space whose dimension grows exponentially with the number of qubits (tensor-products), the QNN operates in a far richer feature space than a classical feed-forward layer of comparable size.
- Superposition allows the quantum circuit to manipulate many basis states simultaneously → potential speedup.
- Entanglement introduces correlations between qubits that cannot be represented by any separable classical model without large weight matrices, allowing the QNN to capture complex joint feature interactions.
- Together, these properties enable the QNN to express highly nonlinear transformations with dramatically fewer parameters and without explicitly storing or multiplying high-dimensional classical weight matrices.

11.2 Results

- Across all four configurations, both the classical and quantum models show steadily decreasing validation perplexity and loss as training progresses.
- While the QNN consistently starts higher and converges more slowly, its curve repeatedly tracks the classical model's trajectory and ends up in a similar range by the later training steps.
- Matching the classical learning trajectory under such severe dimensional constraints suggests a potential expressivity-per-parameter advantage, where quantum circuits can represent complex transformations more compactly than their classical counterparts.
- If this behavior scales, it points toward a practical form of quantum advantage: achieving comparable performance using significantly smaller, more efficient models.